Monatshefte für Chemie - Chemical Monthly (2023) 154:141–149
https://doi.org/10.1007/s00706-022-02999-5

ORIGINAL PAPER

Distinction between film loss and enzyme inactivation in protein-film voltammetry: a theoretical study in cyclic staircase voltammetry

Rubin Gulaboski[1]

Received: 19 September 2022 / Accepted: 13 October 2022 / Published online: 27 October 2022

Abstract

Inactivation of redox enzymes and the loss of enzyme's material from its adsorbed film on electrode surface are events that have similar outputs when studied under conditions of protein-film voltammetry. In the current work, we present a series of novel theoretical results under conditions of protein-film cyclic staircase voltammetry that clearly reveal how to distinguish between these two events. Theoretical model elaborated in this work comprises a surface electrode mechanism in which the initial form of redox enzyme is involved in same time in an electrode transformation and in an irreversible reaction of deactivation. While a large set of theoretical voltammetric curves simulated at different conditions are discussed, we also give a tabular overview of some characteristic cyclic voltammetric patterns of this electrode mechanism. The simulated voltammograms can help the experimentalists to distinguish the phenomenon of loss of protein film from the electrode mechanism associated with enzyme deactivation. In addition, we give hints to apply suitable methodologies to get access to the kinetics of both steps involved in this electrochemical mechanism.

Graphical abstract

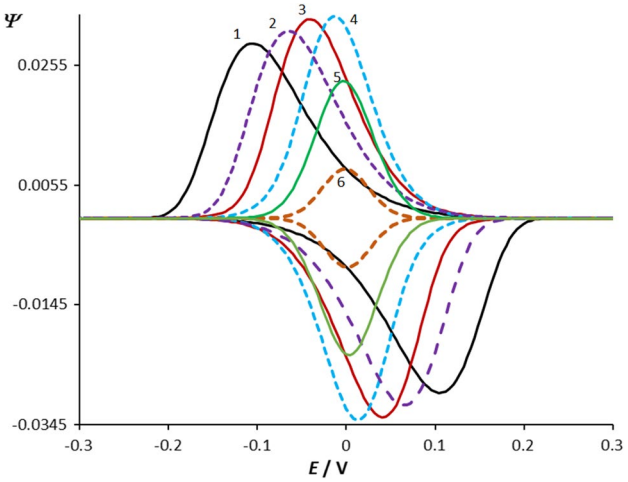

Keywords Protein-film voltammetry · Enzyme inactivation · Kinetic of reaction of enzymatic inactivation · Cyclic voltammetry · Protein-film loss

Introduction

Redox enzymes are the most crucial constituents in various physiological processes related to mass transfers, biochemical synthesis, and energy conversion in all living

✉ Rubin Gulaboski
rubin.gulaboski@ugd.edu.mk

[1] Faculty of Medical Sciences, "Goce Delcev" University Stip, 2000 Stip, Republic of Macedonia

systems [1]. As reported in [2], various chemical reactions and physical processes often lead to inactivation of the redox enzymes under physiological conditions. The complex structure and the flexible chemistry of redox enzymes is main origin of unwanted side reactions that are not related to their major role in defined catalytic reaction. A loss of ligand from the structure around redox active site, and structural changes taking place nearby the active site commonly create an enzymatic structure that will have no further chemical potential to catalyze a defined chemical process. Since many enzymes are major constituents in designing of highly specific electrochemical biosensors [3], the enzymatic inactivation is undesired phenomenon in biotechnology, where a long-lasting activity of the enzymes is aimed to be achieved. From that point of view, it is important to get deeper insight into the electrochemistry of processes of inactivation of redox enzymes. By performing electrochemical experiments designed to understand the inactivation of redox enzymes, one gets relevant set of information about the chemistry and activity of redox enzyme's active sites. In the last 25 years, the protein-film voltammetry (PFV) came out as a simple but very efficient electrochemical methodology that enables deeper insight into the redox features of many lipophilic redox enzymes [5–10]. In this relatively short time since its introduction, the number of redox enzymes studied in PFV has increased enormously [11, 12]. The experiments in PFV are performed in common three-electrode cell, by exploring less than a microgram amount of redox enzyme that keeps activity even after being immobilized at surface of suitable working electrode. Many aspects related to electrochemistry and activity of redox enzymes are already considered theoretically in PFV methodology [13–26]. Only recently, however, our group initiated first theoretical report (under conditions of square-wave voltammetry) considering an electrochemical mechanism in PFV, where the initial electrochemically active form of given redox enzyme is involved simultaneously in an electrode transformation and in an irreversible chemical reaction of deactivation. Indeed, such an electrochemical mechanism is very important since it is often related to the processes of inactivation of many redox proteins [27]. In this work, we present theoretical results of this model under conditions of cyclic staircase voltammetry (CSV). The results elaborated in this work clearly reveal how one can distinguish the enzyme inactivation in elaborated mechanism from the scenario of enzyme loss from the adsorbed film in PFV. While we give set of cyclic voltammograms that will help in recognizing this electrode mechanism, we give the readers hints to develop adequate protocols to get access to all relevant physical parameters involved in this mechanism.

Scheme 1

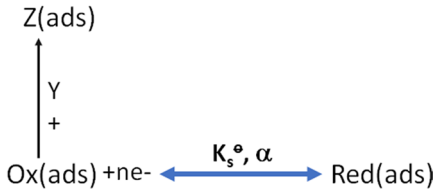

Mathematical model

In the mathematical model, a so-called "surface electrode mechanism" is theoretically elaborated, with oxidized (Ox) species of redox enzyme initially present in electrochemical cell. The molecules of initial redox form "Ox" are assumed to be firmly adsorbed in a form of monolayer at the surface of working electrode. Upon applying a controlled bias between the working and the reference electrode, the initial electrochemically active species Ox(ads) start to get involved in parallel in an electrochemical transformation and in an irreversible chemical reaction of deactivation, as it is portrayed Scheme 1.

While all species Ox, Red, and Z are supposed to be strongly adsorbed ("ads") on the surface of the working electrode, it is additionally assumed that no interactions of any type occur between their adsorbed molecules. Moreover, it is assumed that no mass transfer of any species takes place via diffusion in electrochemical cell. "Y" in Scheme 1 stays to describe a substrate present in excess in electrochemical cell that reacts selectively in irreversible manner only with the molecules of initial redox form Ox(ads). The irreversible chemical reaction with "Y" leads to inactivation of the starting redox form of Ox(ads) species, while electrochemically inactive species Z(ads) are created. Z(ads) is a final product in the chemical reaction between Ox(ads) and "Y", and the molecules of Z(ads) show no electrochemical activity in the region of applied potentials. It is assumed that the concentration of substrate "Y" stays constant near the working electrode surface in the course of voltammetric experiments. Thus, the kinetics of the irreversible inactivation reaction in Scheme 1 is of pseudo-first order. Mathematically, the considered electrode mechanism in Scheme 1 can be described by following equations:

$$[\mathrm{d}\Gamma(\mathrm{Ox})/dt] = -I/(nFS) - k_c\Gamma(\mathrm{Ox}) \quad (1)$$

$$[\mathrm{d}\Gamma(\mathrm{Red})/dt] = I/(nFS) \quad (2)$$

$$[\mathrm{d}\Gamma(\mathrm{Z})/\mathrm{d}t] = k_c\Gamma(\mathrm{Ox}) \quad (3)$$

The differential equations Eq. (1)–(3) were solved under following conditions:

$$t = 0; \Gamma(\mathrm{Ox}) = \Gamma^{*}(\mathrm{Ox}); \Gamma(\mathrm{Red}) = \Gamma(\mathrm{Z}) = 0 \quad (4)$$

$$t > 0; \Gamma(\mathrm{Ox}) + \Gamma(\mathrm{Red}) + \Gamma(\mathrm{Z}) = \Gamma^{*}(\mathrm{Ox}) \quad (5)$$

We assume that the Butler–Volmer formalism applies at the surface of working electrode, having the following form:

$$[I/nFS] = k_{s}\exp(-\alpha\phi)\,[\Gamma(\mathrm{Ox}) - \exp(\phi)\Gamma(\mathrm{Red})] \quad (6)$$

Using the method of Nicholson, Hamilton, and Olmstead [28], a numerical solution of Eq. (6) has been obtained. A detailed MATHCAD file that contains all recurrent formulas and the parameters needed to calculate the dimensionless voltammograms of this electrode mechanism is given in the Supplementary material of this work. The meaning of all symbols and the definitions of all parameters explored in theoretical simulations of this electrode mechanism are: Ψ is a symbol of the dimensionless current defined as $\Psi = I\tau/[(nFS\Gamma^{*}(\mathrm{Ox})]$. In last equation, symbol I stays for the electric current, τ is duration of a single potential step in cyclic staircase voltammetry (τ was set to 0.02 s in all calculations), n is number of electrons exchanged in the electrochemical reaction between the working electrode and the redox forms of the enzyme Ox and Red, F is Faraday constant, S is surface area of working electrode, while $\Gamma^{*}(\mathrm{Ox})$ is the surface concentration of initial enzymatic redox form Ox. $\Gamma(\mathrm{Ox})$, $\Gamma(\mathrm{Red})$, and $\Gamma(\mathrm{Z})$ stay for the surface concentrations of species Ox, Red, and Z, respectively, while $c(\mathrm{Y})$ is symbol of the molar concentration of the substrate "Y". α is symbol of the electron transfer coefficient (α was set to 0.5 in all calculations), R is universal gas constant, while Φ is a symbol of dimensionless potential defined with the equation $\Phi = \frac{nF}{RT}\left(E - E^{\phi'}\right)$. In last equation, E is symbol of the applied potential, while E^{Θ} stays for the standard redox potential of couple Ox(ads)/Red(ads). dE is symbol of the height of potential steps and it was set to 4 mV in all calculations.

If one applies constant instrumental parameters, and at constant temperature T (temperature of 298 K was used in all calculations), the major characteristics of simulated cyclic voltammograms depend mainly on two dimensionless parameters K_{ET} and K_{chem}. K_{ET} is a dimensionless electrode kinetic parameter, and this parameter controls the rate of the electron transfer step. It is defined as $K_{\mathrm{ET}} = k_{s}^{\Theta}\tau$, where k_{s}^{Θ} (s^{-1}) is standard rate constant of electron transfer step. The magnitude of K_{ET} portrays the rate of electron exchange between working electrode and redox adsorbates Ox and Red, relative to time duration (τ) of applied steps in CSV. The magnitude of the dimensionless chemical kinetic parameter K_{chem} (defined as $K_{\mathrm{chem}} = k_{c}\tau$) reflects the rate of irreversible chemical reaction of inactivation of the species Ox(ads) relative to the time duration of potential steps in CSV. It is important to underline that the chemical rate constant k_{c} in last equation is defined as: $k_{c} = k_{c}'$ x $c(\mathrm{Y})$. Here, k_{c}' stays to describe the real chemical rate constant of inactivation of Ox(ads), while $c(\mathrm{Y})$ is the molar concentration of substrate "Y". For calculating the cyclic voltammograms of considered mechanism, we used the commercial software MATHCAD 14. The reduction currents in the mathematical model are defined to be positive, while the reoxidation currents are defined to have negative sign, which is in line with the US electrochemical convention.

Results and discussion

Although there are many theoretical works reporting on different electrode mechanisms coupled with chemical reactions in PFV [12–26, 29–38], so far there had been no theoretical work that considers inactivation of initial redox enzymatic form under conditions of PFV. In voltammetric practice, it is very difficult to discern between the protein irreversible inactivation and the film loss from the adsorbed protein [27]. This is because both events exhibit similar effects in the recorded voltammetric patterns. To get impression about overall behavior of the systems of interest, we start in this part with short elaboration of initial theoretical voltammetric results of considered mechanism (I) obtained almost in absence of inactivation reaction. As expected, if the rate of the chemical step in considered mechanism is very small (i.e., $K_{\mathrm{chem}} < 0.005$), then one obtains cyclic voltammograms as of a simple surface electrode mechanism [4, 5, 8, 39]. Shown in Fig. 1 is a series of cyclic staircase voltammograms calculated at several rates of the electron transfer step. Remarkably, the magnitude of K_{ET} affects all relevant features of the cyclic voltammograms, i.e., the peak heights, the position of the cathodic and anodic peaks, and the peak-to-peak potential separation as well. An increase of the dimensionless electrode kinetic parameter K_{ET} leads to shift of the peak potentials of cathodic peaks to more positive potentials and shift of the anodic peaks toward more negative potentials. For $\log(K_{\mathrm{ET}}) > -0.3$, both cathodic and anodic peaks are positioned at identical potential of 0.00 V, which coincides with the standard potential of redox couple Ox/Red defined in the simulation protocol. Any further increase of K_{ET} does not induce changes in the positions of both cathodic and anodic peaks. Shown in Fig. 2a are the dependences between the cathodic ($E_{\mathrm{c,p}}$) and anodic ($E_{\mathrm{a,p}}$) peak potentials as a function of $\log(K_{\mathrm{ET}})$. In both cases, in the region of small rates of the kinetic of electron transfer, i.e. $-3 < \log(K_{\mathrm{ET}}) < -1$, there is linear dependence between $E_{\mathrm{c,p}}$ and $E_{\mathrm{a,p}}$ vs. $\log(K_{\mathrm{ET}})$, with slopes of those dependences equal to $\pm 2.303RT/(\alpha nF)$, correspondingly. The last equation enables estimation of electron transfer coefficient α from experiments in which position of cathodic or anodic peaks will be determined at different scan rates [5, 39]. The

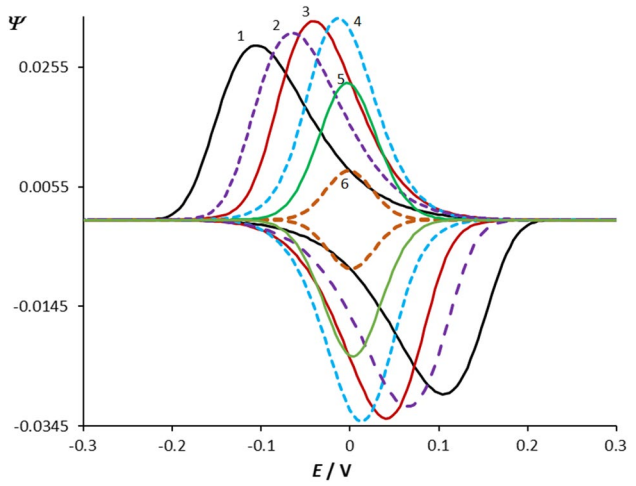

Fig. 1 Cyclic staircase voltammograms of considered surface electrode mechanism associated with irreversible chemical inactivation of initial redox enzymatic form. Voltammograms are calculated at small rate of chemical reaction ($K_{chem}=0.0001$), and they display the effect of the dimensionless electrode kinetic parameter K_{ET}. Other simulation conditions were: temperature $T=298$ K, number of electrons exchanged $n=1$, electron transfer coefficient $\alpha=0.5$, height of potential step $dE=4$ mV, duration of potential steps $\Gamma=0.02$ s. The magnitudes of the dimensionless electrode kinetic parameter K_{ET} were set to 0.01 (1); 0.025 (2); 0.05 (3); 0.20 (4); 0.80 (5), and 2.0 (6). Starting potential in was set to + 0.30 V and scans were running toward final potential of − 0.30 V

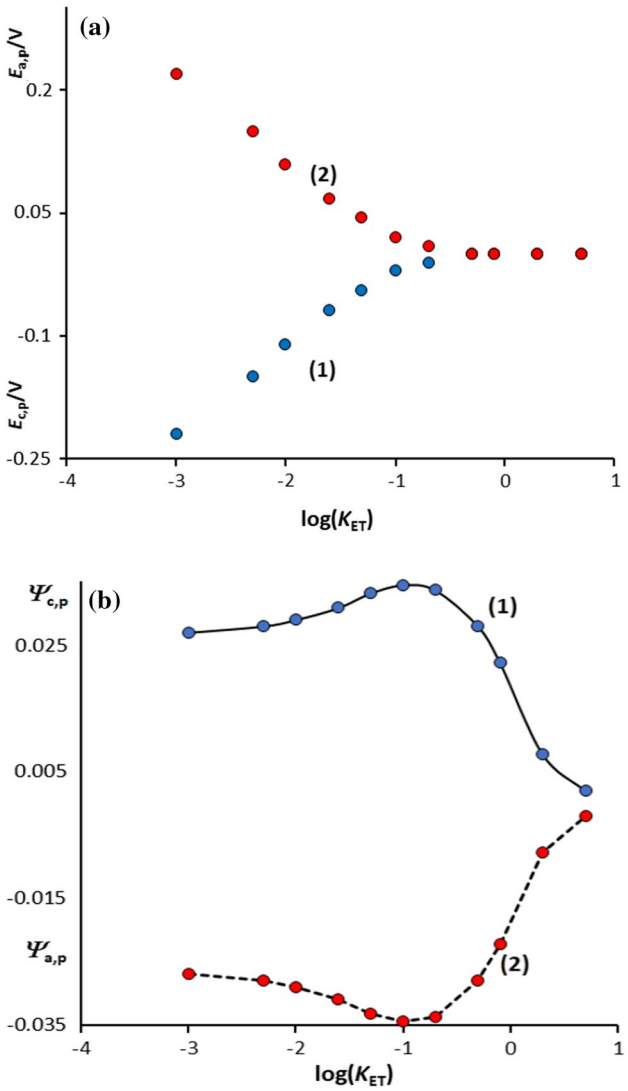

Fig. 2 **a** Dependences of the cathodic (1) and anodic (2) peak potentials of simulated curves as those represented in Fig. 1 as a function of log(K_{ET}); **b** dependences of the cathodic (1) and anodic (2) peak currents as a function of log(K_{ET}). Starting potential was set to + 0.50 V and scans were running toward final potential of − 0.50 V. Other simulation conditions were same as those reported in Fig. 1

dependences between the currents of the cathodic and anodic peaks as a function of log(K_{ET}) is presented in Fig. 2b. The parabolic dependences existing at both curves in Fig. 2b are due to specific chrono-amperometric features of surface electrode mechanisms in step or pulse voltammetry [29, 30]. In pulse voltammetric techniques, this feature is commonly known as "quasireverasible maximum" [30]. Due to synchronization between the rate of electron transfer step and the time-frame in which current is measured in step or pulse voltammetric techniques, electrochemical reactions characterized with moderate rate of electron transfer exhibit much higher peak currents. Oppositely, the surface redox systems featuring very fast electron transfer exhibit much lower voltammetric peak currents in pulse and step techniques (see curves 5 and 6 in Fig. 1, for example) [29, 30, 39]. Since the maxima of the parabolas in Fig. 2b correspond to certain critical values of K_{ET}, one can use this phenomenon to get access to standard rate constant of electron transfer k_s^e following the procedure described elsewhere [30]. As it has been mentioned in "Introduction", common event taking place in protein-film voltammetry methodology is the loss of the protein film from the electrode surface [27]. Shown in Fig. 3 is one voltammetric example of loss of the protein from the immobilized film. If one makes consecutive voltammetric scans, destruction of the film of adsorbed protein is portrayed in subsequent lowering of the intensities of both cathodic and anodic peaks, while the position of both peaks remains unaltered (see Fig. 3) [27]. Similar features are also expected to happen in case of inactivation of the initial electrochemically active form of redox enzymes studied in PFV. As we will see, however, the voltammetric outputs of enzyme inactivation in considered mechanism in this work have quite distinctive features than that resulting of film loss displayed in Fig. 3. A series of cyclic voltammograms, calculated at several distinct values of K_{ET} and K_{chem} are displayed in Table 1. The voltammograms in first two rows of Table 1 are calculated at slow rates of electron transfer step, while those placed in the third and fourth rows feature

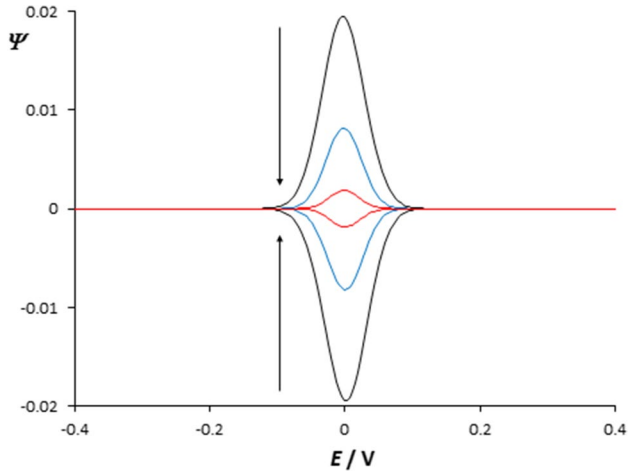

Fig. 3 Effect of consecutive scanning to the features of simulated cyclic voltammograms in case of enzyme loss of the adsorbed film in PFV. Every consecutive scan in direction of the arrows leads to lower currents detected, while position of both peaks remains unaltered. In this set of simulations, the surface concentration of initial redox protein Ox is the only variable. It gets lower magnitude for each consecutive scan starting from the black curve and going toward red curve in direction of the current diminishment presented at cyclic voltammograms, which corresponds to the film loss in PFV methodology

moderate and fast rate of electron transfer steps, respectively. In all cases, by going from the far left to the far right voltammogram, the magnitude of dimensionless chemical parameter K_{chem} increases. The voltammetric curves placed in first left column are calculated at negligible rates of the irreversible chemical reaction, so their shapes are typical as of undisturbed simple surface electrochemical mechanism [5, 39].

For slow rate of electron transfer step (voltammograms in the first two rows of Table 1), the rate of chemical reaction of inactivation starts to show effects to the features of cyclic voltammograms for magnitudes of $K_{chem} > 0.1$. From chemical point of view, it should be underlined that the chemical reaction removes the initial electrochemically active form of studied redox enzyme. Consequently, it is intuitively expected that lower voltammetric currents will be detected by increasing of chemical rate parameter. This really happens for chemical rates described by $K_{chem} > 0.1$, if $K_{ET} < 0.01$.

Next to this characteristic, and if $K_{ET} < 0.01$, three more voltammetric features are worth to be pointed out, obtained under the influence of rate of irreversible chemical reaction at $K_{chem} > 0.1$: (a) the reoxidation (anodic) peak decreases by an increase of $K_{chem} > 0.1$, but it retains its shape at all values of K_{chem}; (b) the intensity of reduction (cathodic) peak also decreases if $K_{chem} > 0.1$, but it starts to exhibit plateau-like shapes at chemical inactivation rates characterized with $K_{chem} > 0.50$; (c) both peaks shift to more positive potentials by increasing the chemical rate, roughly at $K_{chem} > 0.10$. The plateau-like shape of the cathodic current component is characteristic feature met by CE mechanism [29, 39], while the shift of position of both peaks toward more positive potential by an increase of K_{chem} is a feature typical of EC mechanisms [39]. If we compare the features of voltammograms in first two rows of Table 1 with the voltammograms representing film loss in Fig. 3, it is quite clear that fundamental differences exist between these two electrode mechanisms. At this point, it should be pointed out that the plateau-like shapes of cathodic current components, observed under increased rate of chemical reaction, appear due to the permanent consumption of the Ox(ads) species that takes place in the time-frame of current-sampling fragment of potential steps in CSV [30, 35]. In case of moderate rate of electron transfer step (voltammograms in third row, simulated at $K_{ET} = 0.10$), one observes similar features as those described for the voltammograms in first two rows. If $K_{ET} = 0.10$, for example, then the plateau-like shape of the cathodic current component starts to appear at higher rates of the chemical reaction, i.e., at $K_{chem} \geq 10$.

What happens to cyclic voltammograms under the influence of rate of irreversible chemical reaction of inactivation, if the rate of electron transfer step is large

If the rate of electron exchange between the redox adsorbates Ox and Red with the working electrode surface is large (roughly at $K_{ET} \geq 0.75$), then one observes a series of atypical phenomena in simulated cyclic voltammograms. Shown in the fourth row of Table 1 are cyclic voltammograms, calculated at $K_{ET} = 1.80$, and for several magnitudes of K_{chem}. If the rate of the chemical reaction falls in the region $1 < K_{chem} < 10$, then one observes a simultaneous increase (and not decrease) of the intensity of both peaks as the rate of chemical reaction increases (compare the currents of first two voltammograms from the left in the fourth row of Table 1, for example). Further increase of K_{chem} leads to decrease of the intensity of both current components, while the plateau-like shape at the cathodic peak appears at larger rates of chemical reaction (at $K_{chem} > 200$ in this scenario). A more detailed representation of the effect of K_{chem} to the cyclic voltammograms featuring large rate of electron transfer step is given in Fig. 4a–b. In this part of the work, we give a short explanation that can give hints to understand behavior of voltammetric curves displayed in Fig. 4a, and those placed in the fourth row of Table 1 as well. To understand this atypical behavior in cyclic voltammograms, one should be aware of the specific chrono-amperometric features of surface electrochemical reactions featuring fast electron transfer rate when studied in pulse or step voltammetric

Table 1 Reduction (cathodic) and reoxidation (anodic) current components of cyclic staircase voltammograms calculated at different rates of electron transfer step and at several rates of irreversible chemical reaction of inactivation

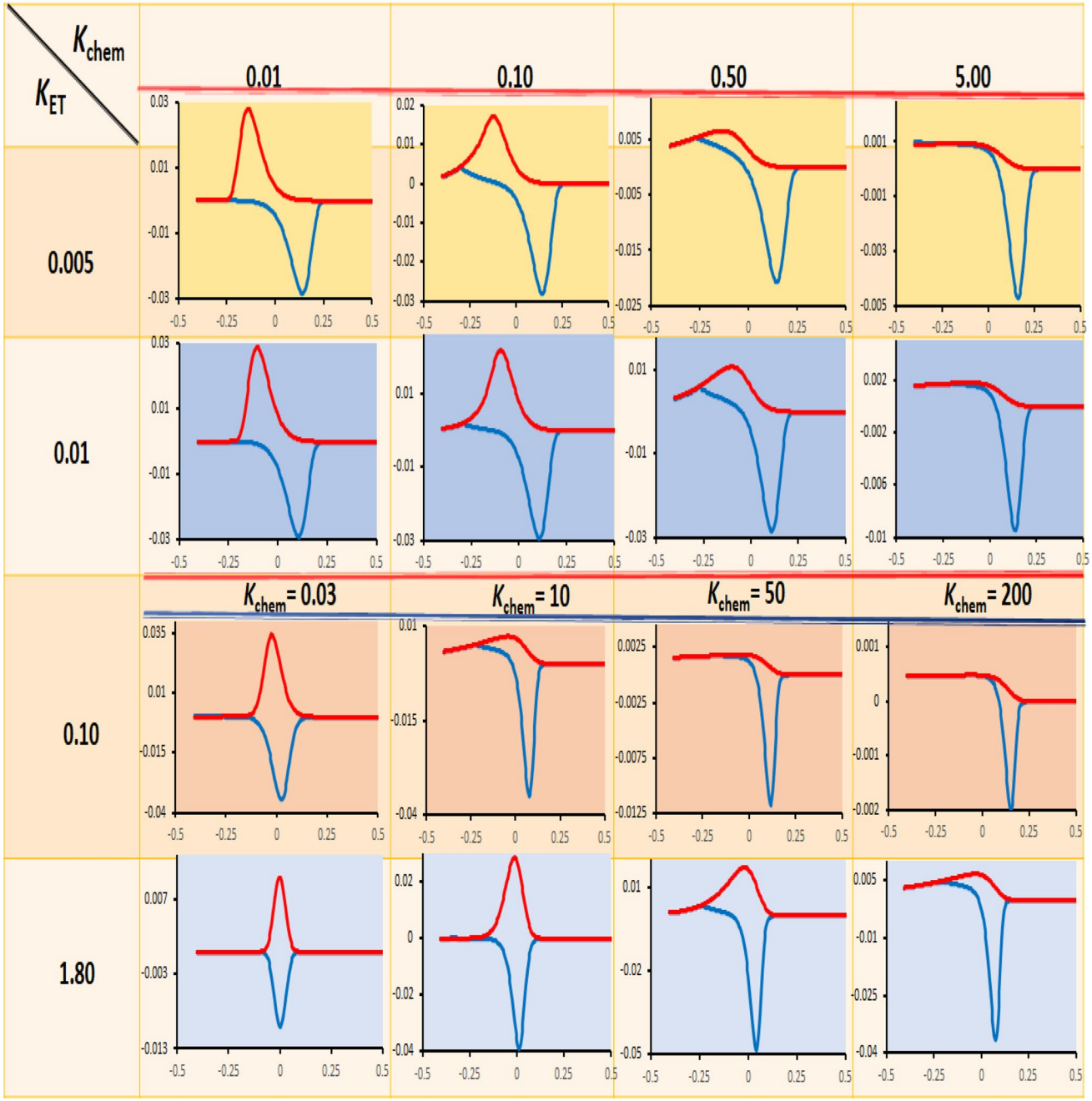

For all curves presented in this table, a potential step of 4 mV was used, while the electron transfer coefficient in all simulations was set to $\alpha = 0.5$. Starting potential was set to + 0.5 V and the forward (cathodic) scans run from + 0.5 V to final potential of − 0.4 V. *E*/V is on all *x*-axes, while dimensionless current Ψ is on *y*-axes of all voltammograms

techniques [30]. Due to the fast rate of electron exchange, most of the Ox(ads) species convert electrochemically to Red(ads) species at the beginning of the applied potential steps, i.e., in the so-called "dead-time". Since the current in cyclic staircase voltammetry is sampled in a small time-fragment at the end of potential steps [29, 30], a rather small amount of the initial redox form Ox(ads) will remain to undergo electrochemical transformation there. However, when Ox(ads) species get engaged in a simultaneous chemical reaction of irreversible inactivation, then moderate rates of the chemical step might significantly disturb the equilibrium of electrochemical reaction Ox(ads) + *n*e- ↔ Red(ads) that happens in the "dead-time" of potential steps. This phenomenon will

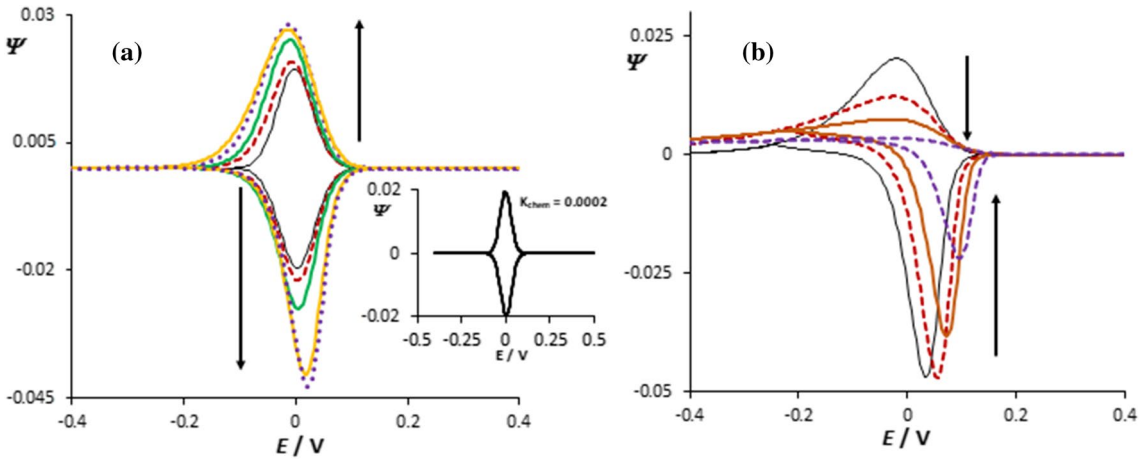

Fig. 4 Cyclic staircase voltammograms of considered electrochemical mechanism in which the initial enzymatic redox form is also involved in chemical reaction of inactivation. All voltammograms were calculated at $K_{ET}=1.0$, and they represent the effect of dimensionless chemical rate parameter K_{chem}. The magnitudes of the dimensionless chemical kinetic parameter K_{chem} were set to 0.0002; 1.0; 2.0; 5.0; and 10.0 (from the curve with lowest to the curve with highest peak currents in direction of arrows in pattern (**a**), while the values of K_{chem} were 20; 50; 100; and 250 in direction of the arrows in pattern (**b**). Starting potential was set to + 0.40 V and scans were running toward final potential of − 0.40 V. Other simulation conditions were same as those reported in Fig. 1

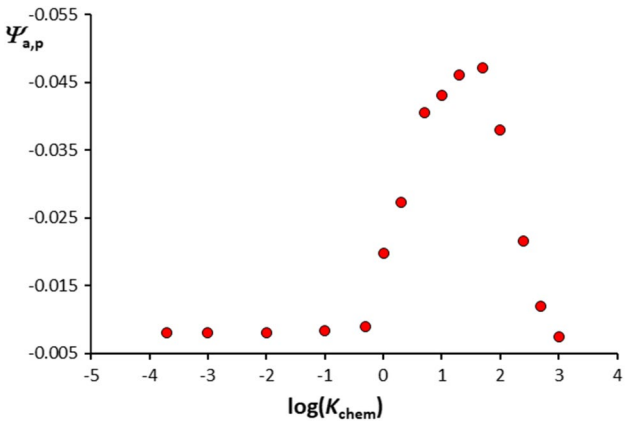

Fig. 5 Dependence of anodic peak currents of the cyclic voltammograms in Fig. 4 as a function of $\log(K_{chem})$. Other simulation conditions were same as those reported in Fig. 4

allow more Ox(ads) species to remain available for electrochemical transformation in the time-frame of potential steps where current is sampled. As a consequence, a current increase in region of moderate rates of chemical step is detected, as displayed in voltammograms in Fig. 4a. In such scenario, one observes concomitant decrease of both current components, and appearance of plateau-like shapes at the cathodic current component at significant rates of the chemical step defined by $K_{chem} > 50$ (Fig. 4b). In scenario of large values of K_{ET}, a nicely expressed parabolic dependence exists between the anodic peak currents as a function of $\log(K_{chem})$ (see Fig. 5). The features displayed in Figs. 4 and 5 are typical for this electrode mechanism, and they clearly distinguish the enzymatic inactivation from the voltammetric systems featuring loss of the protein film. Therefore, they can be used as diagnostic criteria to make simple distinction between these two mechanisms.

As it has been mentioned earlier in this work, another feature that is quite specific for this electrode mechanism is the shift of position of both peaks toward more positive potentials by increasing the rate of irreversible chemical reaction. Since cathodic peaks get plateau-like shape at higher rates of the chemical reaction, it is more useful to explore the reoxidation peak for analytical purposes. This is quite suitable approach, because at all magnitudes of K_{chem} the anodic peaks are always well defined, thus allowing precise measurement of their peak potentials. Several dependences between the anodic peak potentials ($E_{a,p}$) vs. $\log(K_{chem})$, calculated at three different magnitudes of K_{ET}, are presented in Fig. 6. In all sigmoidal dependences between $E_{net,p}$ and $\log(K_{chem})$ displayed in Fig. 6, there are linear parts of the curves existing roughly in the regions of chemical rates defined with $0.5 < \log(K_{chem}) < 2.5$. The slopes of those linear parts are almost identical, having values of about 58 mV/$\log(K_{chem})$. The equations of the linear parts of the curves displayed in Fig. 6 read: $E_{a,p}/V = 0.057\ \log(K_{chem}) - 0.052$ V (for $K_{ET} = 1.80$); $E_{a,p}/V = 0.06\ \log(K_{chem}) + 0.008$ V (for $K_{ET} = 0.10$); and $E_{a,p}/V = 0.057\ \log(K_{chem}) + 0.096$ V (for $K_{ET} = 0.01$). The last set of equations corresponding to the linear parts of $E_{net,p}$ vs. $\log(K_{chem})$ dependences in Fig. 6 can be explored for the determination of the rate constant of chemical reaction of inactivation, providing that magnitude of K_{ET} is determined previously.

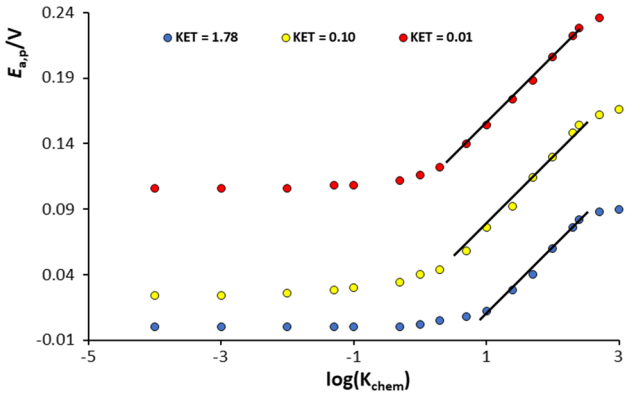

Fig. 6 Dependences of anodic peak potentials ($E_{a,p}$) of cyclic voltammograms of considered electrochemical mechanism as a function of log(K_{chem}). Curves are calculated at three different kinetics of electron transfer step (i.e., three different values of K_{ET}). The magnitudes of the dimensionless kinetic parameter of electron transfer K_{ET} are given in the graph. Other simulation conditions were same as those reported in Fig. 1

Conclusions

While the loss of protein film and irreversible enzymatic inactivation are often encountered in PFV experiments [27], there has been a general opinion that these two phenomena are hardly distinguishable under voltammetric conditions. As elaborated elsewhere [27], anaerobic inactivation Ni–Fe hydrogenases [40–42], nitrate-reductases inactivation in the presence of excess of nitrates [43], bilirubin oxidases and multi-coper oxidases inactivation initiated in the presence of chlorides [27, 44], horseradish peroxidases inactivation in the presence of huge concentrations of hydrogen peroxide [45], and oxidative inactivation of FeFe hydrogenases [46] are just some examples of common inactivation reactions studied in PFV. In this work, via assessing the chemical activity of initial form of redox enzyme that is adsorbed at the surface of working electrode, we created a theoretical background to study irreversible inactivation of initial redox active form in protein-film voltammetry. The features of calculated cyclo-voltammetric curves of this mechanism reveal several specific patterns that can be used to make a clear distinction between the enzymatic inactivation from the phenomenon of film loss in PFV. The plateau-like shape of the cathodic voltammetric current, appearing at large rates of chemical reaction of inactivation can serve as an initial criterion to distinguish the enzymatic inactivation of initial reactant from film loss in PFV. In addition, the shift of both cathodic and anodic peaks to more positive potential under influence of increased chemical reaction rate can also help in recognizing the electrode mechanism associated with enzymatic inactivation. To get advantage of the equations provided to get access to the rate of chemical reaction (Fig. 6), one should avoid of applying scan rate (or time) dependences in corresponding experiments. This is because the time of potential steps in cyclic staircase voltammetry affects simultaneously both kinetic parameters (K_{ET} and K_{chem}) involved in this electrode mechanism. To get access to the parameters of the electron transfer step (α, $k_s^{\ominus}$) in absence of chemical reaction, one might explore protocol reported in Fig. 2 of this work. With the results elaborated in this work, we hope that a nice theoretical basis will be created to help experimentalists in designing proper voltammetric experiments for studying processes of enzymatic inactivation with PFV.

Supplementary Information The online version contains supplementary material available at https://doi.org/10.1007/s00706-022-02999-5.

Acknowledgements Rubin Gulaboski thanks the Alexander von Humboldt Foundation for the support in 2021 during the research stay at the University of Göttingen, Germany.

References

1. Gamenara D, Seoane GA, Saenz-Méndez P, Domínguez de María P (2013) Redox biocatalysis: Fundamentals and applications, John Wiley & Sons
2. Van Loey A, Indrawati SC, Hendrickx M (2002) Inactivation of enzymes: from experimental design to kinetic modeling. In: Whitaker JR, Voragen AGJ, Dominic WS (eds) Handbook of food enzymology. CRC Press, New York
3. Ronkainen NJ, Halsall HB, Heinemann WR (2010) Chem Soc Rev 39:1747
4. Arsmstrong FA (2015) Electrifying metalloenzymes. In: Cho AE, Goddar WA III (eds) Metalloproteins: Theory, calculations and experiments. CRC Press, New York
5. Armstrong FA (1997) Applications of voltammetric methods for probing the chemistry of redox proteins. In: Lenaz G, Milazz G (eds) Bioelectrochemistry: Principles and practice. Birkhauser Verlag AG, Basel
6. Jenner LP, Butt JN (2018) Curr Opin Electrochem 8:81
7. Vincent KA, Parkin A, Armstrong FA (2007) Chem Rev 107:4366
8. Fourmond V, Leger C (2020) An introduction to electrochemical methods for the functional analysis of metalloproteins. In: Crichton RR, Louro RO (eds) Practical approaches to biological inorganic chemistry. Elsevier, Amsterdam, p 325
9. Hirst J (2006) Biochim Biophys Acta Bioener 1757:225
10. Legler C, Bertrand P (2008) Chem Rev 108:2379
11. Chen H, Simoska O, Lim K, Grattieri M, Yuan M, Dong F, Lee YS, Beaver K, Weliwatte S, Gaffney EM, Minteer SD (2020) Chem Rev 120:12903
12. Gulaboski R, Mirceski V (2020) Maced J Chem Chem Eng 39:153
13. Gulaboski R, Mirceski V, Bogeski I, Hoth M (2012) J Solid State Electrochem 16:2315
14. Gulaboski R (2009) J Solid State Electrochem 13:1015
15. Lopez-Tenes M, Gonzalez J, Molina A (2014) J Phys Chem C 118:12312
16. Gulaboski R, Kokoskarova P, Mitrev S (2012) Electrochim Acta 69:86
17. Zhang H-N, Guo Z-Y, Gai P-P (2009) Chin J Anal Chem 37:461
18. Gonzalez J, Lopez-Tenes M, Molina A (2013) J Phys Chem C 117:5208
19. Mann MA, Bottomley LA (2015) Langmuir 31:9511

20. Stevenson GP, Lee C-Y, Kennedy GF, Parkin A, Baker RE, Gillow K, Armstrong FA, Gavaghan DJ, Bond AM (2012) Langmuir 28:9864
21. Fourmond V, Wiedner ES, Shaw WJ, Léger C (2019) J Am Chem Soc 141:11269
22. González J, Sequí J-A (2021) ChemCatChem 13:747
23. Léger C, Elliott SJ, Hoke KR, Jeuken LJC, Jones AK, Armstrong FA (2003) Biochemistry 42:8653
24. Gulaboski R, Mirceski V, Lovric M (2019) J Solid State Electrochem 23:2493
25. Janeva M, Kokoskarova P, Maksimova V, Gulaboski R (2019) Electroanalysis 31:2488
26. Winkler JR, Gray HB (2014) J Am Chem Soc 136:2930
27. del Barrio M, Fourmond V (2019) ChemElectroChem 6:4949
28. Olmstead ML, Hamilton RG, Nicholson RS (1969) Anal Chem 41:260
29. Molina A, Gonzales J (2016) Pulse voltammetry in physical electrochemistry and electroanalysis. In: Scholz F (ed) Monographs in Electrochemistry. Springer, Berlin
30. Mirceski V, Komorsky-Lovric S, Lovric M (2007) Square-wave voltammetry: Theory and application. In: Scholz F (ed) Monographs in Electrochemistry. Springer, Berlin
31. Gulaboski R, Mirceski V (2015) Electrochim Acta 167:219
32. Waskasi MM, Martin DR, Matyushov DV (2018) J Phys Chem B 122:10490
33. Blumberger J (2015) Chem Rev 115:11191
34. Gulaboski R, Mirceski V, Lovric M, Bogeski I (2005) Electrochem Commun 7:515
35. Gulaboski R (2019) Electroanalysis 31:545
36. Guziejewski D, Mirceski V, Jadresko D (2015) Electroanalysis 27:67
37. Jadresko D, Guziejewski D, Mirceski V (2018) ChemElectroChem 5:187
38. Gulaboski R, Lovric M, Mirceski V, Bogeski I, Hoth M (2008) Biophys Chem 137:49
39. Compton RG, Banks CE (2018) Understanding Voltammetry, 3rd edn. World Scientific
40. de Lacey AL, Hatchikian EC, Volbeda A, Frey M, Fontecilla-Camps JC, Fernandez VM (1997) J Am Chem Soc 119:7181
41. Lubitz W, Ogata H, Rüdiger O, Reijerse E (2014) Chem Rev 114:4081
42. Shomura Y, Yoon KS, Nishihara H, Higuchi Y (2011) Nature 479:253
43. Fourmond V, Sabaty M, Arnoux P, Bertrand P, Pignol D, Leger C (2010) J Phys Chem B 114:3341
44. de Poulpiquet A, Kjaergaard CH, Rouhana J, Mazurenko I, Infossi P, Gounel S, Gadiou R, Giudici-Orticoni MT, Solomon EI, Mano N, Lojou E (2017) ACS Catal 7:3916
45. Dequaire M, Limoges B, Moiroux J, Savéant JM (2002) J Am Chem Soc 124:240
46. Rodríguez-Maciá P, Reijerse EJ, van Gastel M, DeBeer S, Lubitz W, Rüdiger O, Birrell JA (2018) J Am Chem Soc 140:9346